

Parametric identification of the non-linear model of a Blumlein N₂-laser

T. Niewierowicz, L. Kawecki, and J. de la Rosa

*Sección de Estudios de Posgrado e Investigación, Escuela Superior de Ingeniería Mecánica y Eléctrica
Instituto Politécnico Nacional
07738 México, D.F., Mexico*

Recibido el 7 de octubre de 1997; aceptado el 17 de septiembre de 1998

In this work we propose a non-linear model of the Blumlein circuit for the excitation of a N₂-laser that produces a high order integro-differential equations system, when each of the two discharges (the spark gap and the laser chamber) taking place in the circuit are simulated by an inductance and a resistance connected in series. The inductance and the resistance of each discharge are considered current dependent and their time behavior is found by means of a parametric identification method based in the measured voltages in the charge capacitors. A Runge-Kutta method to solve the integral terms and a Gauss-Seidel algorithm for the parametric identification were used.

Keywords: Lasers; electrical discharges; parametric identification

En este trabajo se propone un modelo no lineal del circuito Blumlein para la excitación de un láser de N₂, el cual produce un sistema de ecuaciones integro-diferenciales de alto orden, cuando la descarga de interruptor de chispa (spark gap) y de la cámara de descarga láser se simulan cada uno por medio de una inductancia y una resistencia conectadas en serie. Estas inductancias y resistencias se consideran dependientes de las corrientes respectivas, que a su vez dependen del tiempo. Las dependencias temporales se encuentran usando un método de identificación paramétrica basado en los voltajes medidos en los capacitores de carga. Los términos integrales se resuelven usando el método de Runge-Kutta y la identificación paramétrica se hace usando el algoritmo de Gauss-Seidel.

Descriptores: Lasers; descargas eléctricas; identificación paramétrica

PACS: 42.55

1. Introduction

For the pulsed excitation of N₂, a well known circuit is the Blumlein arrangement (Fig. 1). Its role is to produce a very intense uniform glow discharge across the laser head during a very short time. The Blumlein circuit consist of two common non-linear elements, a spark gap whose function is to fire the circuit and the laser chamber where the laser discharge takes place. Besides, in order to charge the circuit a coil L parallel to the laser head is used. Traditionally it is supposed that when the spark gap fires, the impedance $j\omega L$ shows so high values, in relation to the other elements, that it is possible to eliminate it from the analysis. So, the circuit is reduced to two loops, which follow a fourth order differential equations for any voltage and current in the circuit, when each discharge taking place in the circuit is simulated by an inductance and a resistance connected in series, whose values are considered time independent. By fitting the analytical solution of these equations to the experimental circuit voltages, it been possible to find out the average values of the resistances and the inductances used to simulate the spark gap and the laser chamber.

The application of such values to the analysis of the equivalent circuit follows some discrepancies between experimental and theoretical voltage forms. So, to have better approximations it is necessary to know the transient evolution of these resistances and inductances [1–3]. Until 1977 [4] the transient evolution of the resistance and inductance in a pulse

discharge had been very scarcely studied. And till now all the proposals to know them are based on the fitting of the measured voltage through the discharge to the voltage solution obtained from the equivalent circuit [4, 5]. Recently, Persephonis *et al.* [6] solved the integrodifferential equations of the Blumlein circuit for the excitation of a N₂ laser through a time-varying linear model, particularly they consider the current equations for the laser and the spark gap as linear during very short time intervals. Because they use discrete components that are interconnected through wires in their experiment they could measure the currents with a fast risetime current viewing resistor. From the experimental currents they obtain their first and second derivatives numerically, which substituted at four very close adjacent time instants (considering that during this short time intervals the resistances and inductances are constant) produce four algebraic equations for the unknown inductances and resistances at the corresponding time interval. Repeating the same procedure for other time intervals and scanning the entire time region of both discharges, the time evolution of their equivalent resistance and inductance can be obtained. In our Blumlein circuit, built on a double-sided cooper circuit board [7], we use flat capacitors closely connected to the laser head, the currents arising here flow along sheets (capacitor plates) rather than along wires. So we use a longitudinal coil [8], which introduces no modification at all in the laser arrangement, to measure the current in the laser head. The current in the spark gap, which was fixed in the middle of a capacitor [7], was

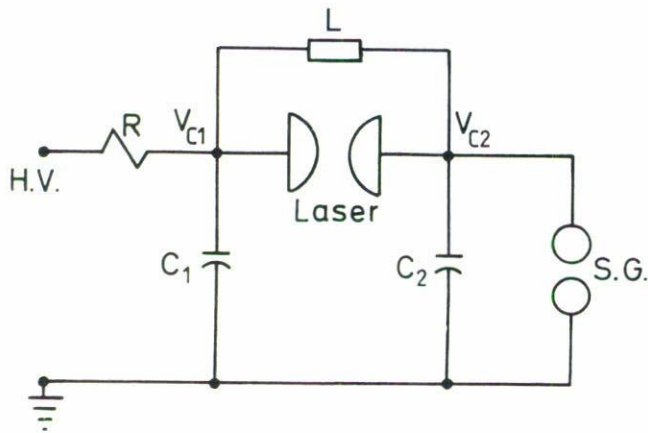


FIGURE 1. Schematic diagram of a Blumlein N₂ laser.

impossible to be measured. The voltages in the circuit are easier to measure, so we write the equation of the voltages for the equivalent circuit. Through a fifth order dependence with the current of the values of the resistance and inductance in the laser head and spark gap loops, the integro-differential equations of the system are solved through a parametric identification method based in the measured voltages in the capacitors C_1 and C_2 . A Runge-Kutta method to solve the integral terms and a Gauss-Seidel algorithm [3] for the parametric identification were used.

2. Theoretical considerations

Figure 1 shows a schematic diagram of the Blumlein circuit. The circuit is composed of a spark gap (S.G.), the laser head, two capacitors and a coil L . When high voltage is applied, both capacitors are equally charged until the breakdown voltage across S.G. is reached. At this potential, the S.G. fires and C_2 begin to discharge very fast through S.G., so does C_1 , but through L and S.G. in a slower way. A very fast rising high voltage difference appears across the laser head until the laser breakdown voltage is reached and the discharge takes place. Figure 2 shows the voltages V_1 and V_2 in the capacitors C_1 and C_2 . The mechanical construction of the laser is reported elsewhere [7].

The voltages V_1 and V_2 were measured with two equal high voltages probes (Tektronix P6015) combined with a 300 Mhz bandwidth oscilloscope (Tektronix 2440). The voltage in the laser head (Fig. 5) is the voltage difference $V_1 - V_2$ which was automatically given by the oscilloscope and is the average of 16 discharges. The current in the laser chamber (Fig. 5) was measured with a home build linear coil [8] and also registered in the oscilloscope. Stable operation of the laser was achieved at voltages ranging from 6 to 12 KV, pressures between 60 and 130 hPa and frequencies up to 20 Hz. The pulse-to-pulse fluctuations of the laser head voltage were fewer than 5%.

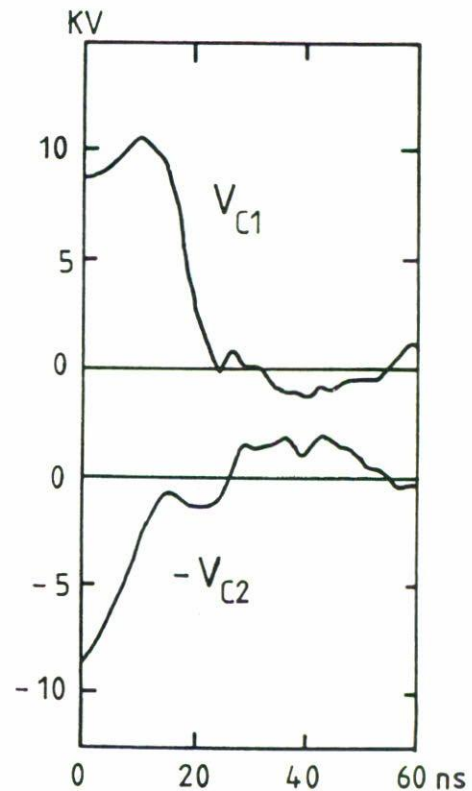


FIGURE 2. From top to bottom: -Voltage appearing in $C_1(V_{C1})$; -voltage in $C_2(V_{C2})$.

To analyze the circuit, each discharge taking place in the circuit is simulated by a non-linear inductance and resistance connected in series (Fig. 3). R_1 and L_1 stand for the inductance and a resistance associated with the laser head loop, respectively, and R_2 and L_2 stand for the analogous parameters of the spark gap loop.

Because the laser and the spark gap change from a non-conducting state to a short circuit, the time dependence of R_1 and R_2 is obvious. The changes in both discharges are due to the change in the electron and ion concentrations, which produce a time and space dependence of their resistivities. As we have in our analysis the currents as state variables, we take R_1 and R_2 as current dependent, where we are considering R_1 (or R_2) as the resistance in the laser loop (or S.G. loop). We propose a form of power series for R_1 (R_2).

Such expansion gives

$$R_1 = f_{R_1}(I_1) = R_{1,p}I_1^p + R_{1,p-1}I_1^{p-1} + R_{1,p-2}I_1^{p-2} + \dots + R_{1,1}I_1 + R_{1,0}, \quad (1)$$

$$R_2 = f_{R_2}(I_2) = R_{2,p}I_2^p + R_{2,p-1}I_2^{p-1} + R_{2,p-2}I_2^{p-2} + \dots + R_{2,1}I_2 + R_{2,0}. \quad (2)$$

With the time change of the spatial distribution of a discharge are related changes in the spatial distribution of the current density $\vec{J} = (\vec{r}, t)$. So the inductance of the discharge, that is function of the dimensions of the conduction volume, is also

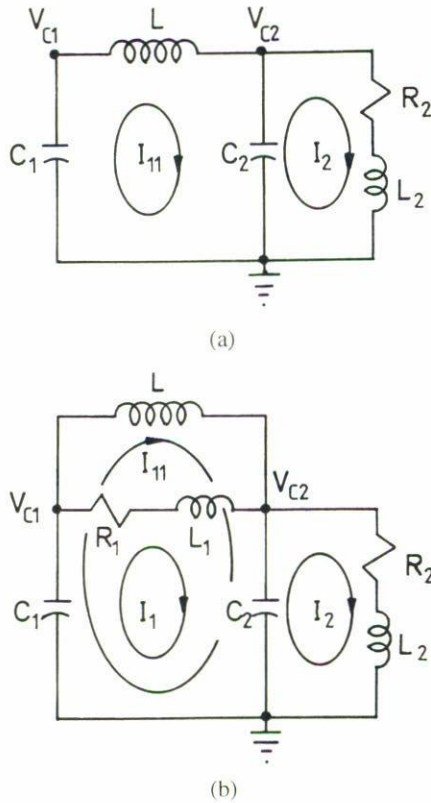


FIGURE 3. Equivalent circuit for the different operation steps of the Blumlein circuit (a) $0 \leq t \leq t_B$, (b) $t_B \leq t \leq t_{FIN}$.

a time dependent function. If $\vec{J} = (\vec{r}, t)$ is not known, then it is not possible to find out the induced magnetic density B , and the inductance L in the discharge can not be calculated.

However we know that the induced electromotive force by the time variation of the current intensity in a loop is given by

$$V = \frac{d\Phi}{dt}, \tag{3}$$

where $\Phi = LI$ is the induced magnetic flux in the loop. Because L and I are time functions, the induced electromotive force can be written as

$$V = \frac{d(LI)}{dt}. \tag{4}$$

In our analysis we are considering the currents in the circuit as state variables, so we take L_1 and L_2 as current dependent.

Besides, if we are considering L_1 (L_2) as the inductance in the laser loop (S.G. loop), we can propose a form of power expansion for L_1 (L_2). Such expansion gives

$$L_1 = f_{L_1}(I_1) = L_{1,p}I_1^p + L_{1,p-1}I_1^{p-1} + L_{1,p-2}I_1^{p-2} + \dots + L_{1,1}I_1 + L_{1,0}, \tag{5}$$

$$L_2 = f_{L_2}(I_2) = L_{2,p}I_2^p + L_{2,p-1}I_2^{p-1} + L_{2,p-2}I_2^{p-2} + \dots + L_{2,1}I_2 + L_{2,0}. \tag{6}$$

The differential equations governing the performance of the circuit are given as follows:

2.1. The first step ($0 \leq t \leq t_B$)

At $t = 0$ the S.G. fires and at $t = t_B$ the laser head fires. Through this step, the equivalent circuit showing the operation of the system is shown in Fig. 3a. The equations governing its performance are given as follows:

$$R_2 I_2 + \frac{d(L_2 I_2)}{dt} + \frac{1}{C_2} \int_0^{t_B} (I_2 - I_{11}) dt + V_2|_{t=0} = 0, \tag{7}$$

$$L \frac{dI_{11}}{dt} + \frac{1}{C_1} \int_0^{t_B} I_{11} dt + \frac{1}{C_2} \int_0^{t_B} (I_{11} - I_2) dt + V_1|_{t=0} + V_2|_{t=0} = 0. \tag{8}$$

2.2. The second step ($t_B \leq t \leq t_{FIN}$)

At t_{FIN} the glow discharge in the laser head gets in the break down. Through this step the equivalent circuit showing the operation of the system is shown in Fig. 3b. The equations governing its performance are given as follows:

$$R_1 I_1 + \frac{d(L_1 I_1)}{dt} + \frac{1}{C_1} \int_{t_B}^{t_{FIN}} (I_1 + I_{11}) dt + V_1|_{t=t_B} + \frac{1}{C_2} \int_{t_B}^{t_{FIN}} (I_1 + I_{11} - I_2) dt + V_2|_{t=t_B} = 0, \tag{9}$$

$$L \frac{dI_{11}}{dt} + \frac{1}{C_1} \int_{t_B}^{t_{FIN}} (I_1 + I_{11}) dt + V_1|_{t=t_B} + \frac{1}{C_2} \int_{t_B}^{t_{FIN}} (I_1 + I_{11} - I_2) dt + V_2|_{t=t_B} = 0, \tag{10}$$

$$R_2 I_2 + \frac{d(L_2 I_2)}{dt} + \frac{1}{C_2} \int_{t_B}^{t_{FIN}} (I_2 - I_1 - I_{11}) dt + V_2|_{t=t_B} = 0. \tag{11}$$

3. Parametric identification

The parametric identification is accomplished through a comparison of the values in the real process and the theoretical model. To do that it is necessary to consider n experimental voltage values for $V_1^*(t_k)$ and for $V_2^*(t_k)$ ($k = 1, 2, \dots, n$), satisfying Eqs. (7) – (11). We have then,

$$V_1 = \frac{1}{C_1} \int_0^t (\alpha I_1 + I_{11}) dt + V_1(0), \tag{12}$$

$$V_2 = \frac{1}{C_2} \int_0^t (I_2 - \alpha I_1 - I_{11}) dt + V_2(0), \tag{13}$$

where

$$\alpha = \begin{cases} 0 & \text{for } 0 \leq t \leq t_B \\ 1 & \text{for } t_B \leq t \leq t_{FIN} \end{cases} \quad (14)$$

and t_B can be obtained from the evaluation of the equation

$$V_B = (V_1 - V_2)|_{t=t_B} = \frac{1}{C_1} \int_0^{t_B} I_{11} dt + V_1|_{t=0} - \frac{1}{C_2} \int_0^{t_B} (I_2 - I_{11}) dt - V_2|_{t=0}, \quad (15)$$

where I_2 and I_{11} are calculated from Eqs. (7) and (8), through a Runge-Kutta method, until Eq. (15) is satisfied for the experimental value of V_B . As parameter identification index we

propose

$$J = \sum_{k=1}^n \left\{ \left[\frac{1}{C_1} \int_0^{t_k} (\alpha I_1 + I_{11}) dt + V_1(0) - V_1^*(t_k) \right]^2 + \left[\frac{1}{C_2} \int_0^{t_k} (I_2 - \alpha I_1 - I_{11}) dt + V_2(0) - V_2^*(t_k) \right]^2 \right\}. \quad (16)$$

To use Eq. (16) we need the values of $R_1, R_2, L_1, L_2, C_1, C_2$. The last ones are established by design, but R_1, R_2, L_1, L_2 , are the non-measurable, non linear resistance and inductance of the laser and spark gap, respectively. We consider them as a p order functions of their current (1)(2) and (5)(6).

The problem is then reduced to the determination of the $4 \times (p + 1)$ parameters $R_{1,i}, R_{2,i}, L_{1,i}, L_{2,i}$, for $i = 0, 1, 2, 3, \dots, p$ that made the value of the Eq. (16) a minimum. In other words we have to obtain,

$$\min_{R_1(I_1), R_2(I_2), L_1(I_1), L_2(I_2)} \sum_{k=1}^n \left\{ \left[\frac{1}{C_1} \int_0^{t_k} (\alpha I_1 + I_{11}) dt + V_1(0) - V_1^*(t_k) \right]^2 + \left[\frac{1}{C_2} \int_0^{t_k} (I_2 - \alpha I_1 - I_{11}) dt + V_2(0) - V_2^*(t_k) \right]^2 \right\}. \quad (17)$$

The currents I_1, I_2 and I_{11} are obtained from the following equations:

$$\alpha \left[\frac{dI_1}{dt} + \frac{R_{1,p}I_1^p + R_{1,p-1}I_1^{p-1} + \dots + R_{1,1}I_1 + R_{1,0}}{B_1} I_1 + \frac{1}{B_1 C_1} \int_0^{t_{FIN}} (I_1 + I_{11}) dt + \frac{1}{B_1} V_1|_{t=0} + \frac{1}{B_1 C_2} \int_0^{t_{FIN}} (I_1 + I_{11} - I_2) dt + \frac{1}{B_1} V_2|_{t=0} \right] = 0, \quad (18)$$

$$\frac{dI_{11}}{dt} + \frac{1}{LC_1} \int_0^{t_{FIN}} (\alpha I_1 + I_{11}) dt + \frac{1}{L} V_1|_{t=0} + \frac{1}{LC_2} \int_0^{t_{FIN}} (\alpha I_1 + I_{11} - I_2) dt + \frac{1}{L} V_2|_{t=0} = 0, \quad (19)$$

$$\frac{dI_2}{dt} + \frac{R_{2,p}I_2^p + R_{2,p-1}I_2^{p-1} + \dots + R_{2,1}I_2 + R_{2,0}}{B_2} I_2 + \frac{1}{B_2 C_2} \int_0^{t_{FIN}} (I_2 - \alpha I_1 - I_{11}) dt + \frac{1}{B_2} V_2|_{t=0} = 0, \quad (20)$$

where

$$B_1 = (p + 1)L_{1,p}I_1^p + pL_{1,p-1}I_1^{p-1} + (p - 1)L_{1,p-2}I_1^{p-2} + \dots + 2L_{1,1}I_1 + L_{1,0}, \quad (21)$$

$$B_2 = (p + 1)L_{2,p}I_2^p + pL_{2,p-1}I_2^{p-1} + (p - 1)L_{2,p-2}I_2^{p-2} + \dots + 2L_{2,1}I_2 + L_{2,0}. \quad (22)$$

4. Proposed algorithm

The following methods are among the most commonly used in parametric identification: cyclic change of the parameter values or coordinate descent method or Gauss-Seidel method; fastest gradient method; fastest start method; shot or Newton-Raphson method; stochastic change of the parameter values.

We have used an algorithm [3] based on the Gauss-Seidel method [9, 10], which consists of changing the value of only one parameter of the Eqs. (1)(2) and (5)(6), holding the other $(p - 1)$ as constants, until the minimal value of the optimization index Eq. (16) for this parameter is obtained. The changes in the parameter values are carried out using an increasing or decreasing constant. All the other parameters are

treated similarly until a first cycle is completed. A second or more cycles could be done, always with smaller increasing or decreasing constant, until the increasing or decreasing constant is lower than a minimal predetermined value. This minimal predetermined constant gives the accuracy of the calculated values. Because the solution of the Eq. (17) needs the solution of the currents in the circuit, each time the parametric identification is done, the current values are obtained solving the mathematical model given by Eqs. (18)–(22), with the resistance and inductance values calculated from Eqs. (1)(2) and (5)(6). The algorithm was written in FORTRAN and a PC Pentium (200 Mhz) was used. The solution take a maximal of 8 hours and is dependent on the initial values of the declared parameters.

TABLE I. Calculated parameter for the fifth order functions used to represent R_1, R_2, L_1 and L_2 .

i	5	4	3	2	1	0
$R_{1,i}$	0	2.72×10^{-16}	1.34×10^{-11}	8.05×10^{-9}	6.94×10^{-5}	1.880
$R_{2,i}$	0	-7.30×10^{-16}	2.05×10^{-11}	-2.63×10^{-8}	-4.42×10^{-5}	1.401
$L_{1,i}$	0	0	0	1.78×10^{-16}	-7.48×10^{-13}	1.46×10^{-9}
$L_{2,i}$	0	0	0	1.20×10^{-15}	7.15×10^{-13}	1.66×10^{-8}

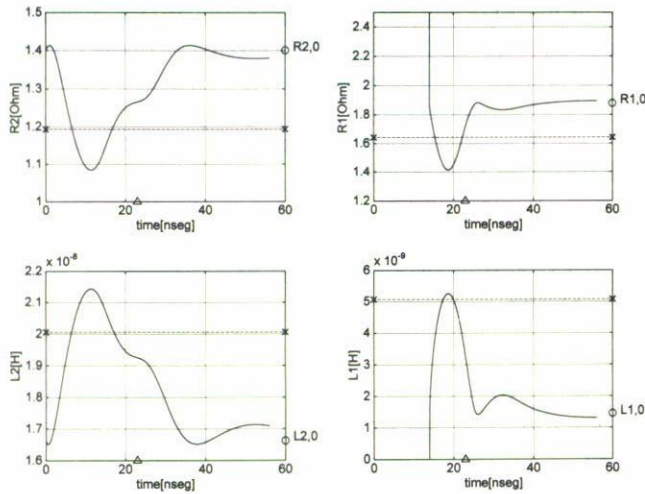


FIGURE 4. Time behavior of the resistance and inductance of the spark gap (R_2, L_2) and of the laser (R_1, L_1) Δ -laser pulse

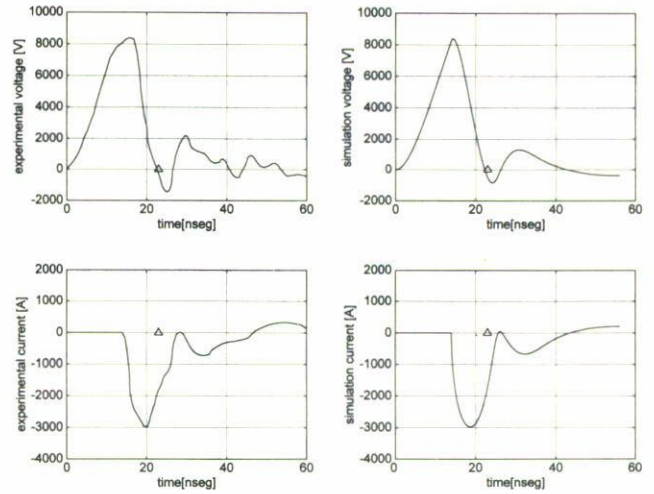


FIGURE 5. Experimental and simulated voltage and current across the laser head Δ -laser pulse.

5. Results and conclusions

While the Persephonis *et al.* model [6] is a time-varying linear model, we introduced here a non-linear one, where the time varying circuit parameters are represented as current functions. The solution of this model produce not only the temporal behavior but the current behavior of these parameters. As a future work it is necessary to investigate if such knowledge can bring out some information about the laser and spark gap discharge. The model could be used in the analysis of other discharge circuits and only needs the measured voltages.

In our study we have considered only the first 60 ns of the discharge, but after laser emission the laser discharge changes into an arc discharge, changing their inductance and resistance drastically. Because this discharge period of time is not interesting for laser emission it has not been analyzed. From the experimental voltage (Fig. 2) we chose 26 values for calculation (see [14]). After processing with V_k, t_k , for $k = 1, 2, \dots, 26$, we obtained the parameter values of the Eqs.(1),(2),(5) and (6) shown in Table I. Figure 4 shows the time behavior of the resistance and inductance of each discharge in the circuit. Finally, Fig. 5 shows the laser voltage and the laser current behavior obtained with the parameter

from Table I and the equations of the circuit. The calculated laser voltage and current in Fig. 5 and the experimental ones show a good fit. Similar time variations of R_1, R_2, L_1 and L_2 in a Blumlein N_2 laser were obtained by Persephonis *et al.* [6].

Following our considerations about R_1, R_2, L_1, L_2 (see Eqs. (1), (2), (5) and (6)) and our experimental arrangement, we could think that the constant values $R_{1,0}, R_{2,0}, L_{1,0}$ and $L_{2,0}$ should be given by the discrete elements of the circuit, *i.e.* C_1, C_2 and the mechanical parts of the laser and the spark gap. But then, from Fig. 4, we see that the resistance both discharges should oscillate between positive and negative values, what is physically impossible.

Statical values of the inductances of C_1 and C_2 can be calculated as follows:

$$L_{C_1} = C_1 Z_0^2, \tag{23}$$

where $C_1 = 3nF$ and Z_0 is given by [11]:

$$Z_0 = \frac{376.7}{\sqrt{\epsilon_r}} \left\{ \frac{\omega}{h} + 0.8825 + 0.1645 \frac{\epsilon_r - 1}{\epsilon_r} + \frac{\epsilon_r}{\pi \epsilon_r} \left[1.4516 + \ln \left(\frac{\omega}{2h} + 0.94 \right) \right] \right\}^{-1} = 0.724 \Omega, \tag{24}$$

where: $\omega = C_1$ width = 38 cm, $h = C_1$ thick = 1.59 mm, $\varepsilon_r = C_1$ dielectric permittivity = 4.6. So $L_{C_1} = 1.57$ nH, which is in the order of $L_{1,0}$.

For L_{C_2} [12]

$$L_{C_2} = \frac{\varepsilon\mu}{2C_2} = 8.5 \text{ nH}, \quad (25)$$

where $\mu = \mu_0$, $\varepsilon = 4.6\varepsilon_0$, and $C_2 = 3$ nF.

From the spark gap geometry, and considering it as a coaxial cable

$$L_{S.G.} = \frac{\mu_0 l}{2\pi} \ln \frac{D}{d} = 8.4 \text{ nH}, \quad (26)$$

where: l = spark gap length = 4 cm, d = external diameter of the spark gap electrodes = 1.4 cm, D = internal diameter of the spark gap chamber = 4 cm. So $L_{C_2} + L_{S.G.} = 16.9$ nH, which is in the order of $L_{2,0}$.

We conclude that $L_{1,0}$ and $L_{2,0}$ are just the inductances given by the construction parameters of the laser arrangement, being the time dependent part of L_1 and L_2 the inductances of the discharges, (i.e. $L_{\text{laser}} = L_{1,2}I_1^2 + L_{1,1}I_1 + L_{1,0}$ and $L_{S.G.} = L_{2,2}I_2^2 + L_{2,1}I_2 + L_{2,0}$, see Table I). For the static values of the resistance of C_1 and C_2 we have to consider only the resistive effect of their cooper electrodes and the dielectric losses equivalent resistances of each capacitor. However this values are small enough when they are compared with $R_{1,0}$ and $R_{2,0}$ (e.g. $R_{C_1} = (2\rho_{C_u}l/A + Z_0 \tan\delta) \simeq 0.0145 \Omega$, where $\rho_{C_u} = 1.78 \times 10^{-6} \Omega\text{cm}$, $l = 27$ cm, $A = 30 \mu\text{m} \times 38$ cm, $\tan\delta = 0.019$ [13] and

$z_0 = 0.724 \Omega$). We conclude then that the values of R_1 and R_2 as a function of the time given in Fig. 4 are correspondent to the ones of the laser discharge and the spark gap discharge.

The physical meaning of all the elements used in our approximation, see Eqs. (1), (2), (5), and (6) and Table I (except $L_{1,0}$ and $L_{2,0}$), is beyond the scope of this work. The temporal behavior of the parameters given in Fig. 4 is discussed in a qualitative way by Persephonis *et al.* [6], arguing avalanche multiplication and Laplace forces.

In Fig. 4 are drawn (pointed lines) the average values we reported in reference [14], where we used a linear equation system in our analysis. We can see that such values are in the range of the obtained in this work. Our new model fit in a better way the measured voltages and with a good confidence the experimental current in the laser (Fig. 5) Comparing our results with the Persephonis [6] ones, we see that our calculated inductances L_1 and L_2 in the circuit are lower. We can explain that if we consider that our arrangement is a compact one built on a doubled-sided cooper circuit board, while Persephonis *et al.* use comercial ceramic capacitors in parallel connected. The conexions in the circuit through cables are responsible for their higher inductances. Our calculated resistances R_1 and R_2 are higher than the Persephonis ones. For the spark gap we use one which works with overvoltages at atmospheric pressure, while Persephonis *et al.* use a triggered pressurized one. For the laser we use a non-preionized laser discharge, while Persephonis *et al.* use a corona preionized one, having in that way lower resistive discharges.

1. P. Persephonis, *J. Appl. Phys.* **62** (1987) 2651.
2. P. Persephonis *et al.*, *IEEE, J. Quantum Electron* **29** (1993) 2371.
3. T. Niewierowicz, L. Kawecki, and J. de la Rosa, *Rev. Mex. Fís.* **41** (1995) 822.
4. T.P. Sorensen, V.M. Ristic, *J. Appl. Phys.* **40** (1977) 114.
5. P. Persephonis, V. Giannetas, A. Ioannon, and J. Parthenios, *J. Appl. Phys.* **43** (1995) 6226.
6. P. Persephonis *et al.*, *IEEE Trans. Plas. Sci.* **24** (1996) 1208.
7. A. Vázquez Martínez, and V. Aboites, *IEEE, J. Quantum Electron* **29** (1993) 2364.
8. J. de la Rosa *et al.*, *Meas. Sci. Technol.* **5** (1994) 1109.
9. D.G. Luenberger, *Linear and Nonlinear Programming*, (Addison-Wesley Publishing Company, 1984).
10. N.S. Bakhvalov, *Numerical Methods*, (MIR 1977), Chap. 6.
11. R.P. Owens, *The Radio and Electronic Engineer* **46** (1976) 360.
12. F.B.J. Leferink, *Proc. 1995 IEEE Int. Symp. Electromag. Comp.*, p. 16.
13. Ch.G. Henningsen, in *Printed Circuits Handbook*, edited by C.F. Coombs, (Mc. Graw-Hill, Inc. 1979), Chap. 2.
14. L. Kawecki, T. Niewierowicz, and J. de la Rosa, *Rev. Mex. Fis.* **43** (1997) 248.